MOLECULAR AND CELLULAR BIOLOGY, Mar. 2008, p. 2035–2046 Vol. 28, No. 6
0270-7306/08/$08.00+0 doi:10.1128/MCB.01770-07

Phosphorylated YDXV Motifs and Nck SH2/SH3 Adaptors Act Cooperatively To Induce Actin Reorganization▽

Ivan M. Blasutig,[1,2] Laura A. New,[3] Ajitha Thanabalasuriar,[4] Thamara K. Dayarathna,[5] Marilyn Goudreault,[1] Susan E. Quaggin,[1,6,7] Shawn S.-C. Li,[5] Samantha Gruenheid,[4] Nina Jones,[3] and Tony Pawson[1,2]*

Samuel Lunenfeld Research Institute, Mount Sinai Hospital, 600 University Avenue, Toronto, Ontario M5G 1X5, Canada[1]; Department of Molecular and Medical Genetics, 4388 Medical Sciences Building, 1 King's College Circle, University of Toronto, Toronto, Ontario M5S 1A8, Canada[2]; Department of Molecular and Cellular Biology, University of Guelph, Guelph, Ontario N1G 2W1, Canada[3]; Department of Microbiology and Immunology, Lyman Duff Medical Building, 3775 University St., McGill University, Montreal, Quebec H3A 2B4, Canada[4]; Department of Biochemistry, Schulich School of Medicine, Faculty of Medicine and Dentistry, University of Western Ontario, London, Ontario N6A 5C1, Canada[5]; Institute of Medical Science, 7213 Medical Sciences Building, 1 King's College Circle, University of Toronto, Toronto, Ontario M5S 1A8, Canada[6]; and Division of Nephrology, St. Michael's Hospital, 30 Bond Street, Toronto, Ontario M5B 1W8, Canada[7]

Received 26 September 2007/Returned for modification 2 November 2007/Accepted 4 January 2008

We have analyzed the means by which the Nck family of adaptor proteins couples adhesion proteins to actin reorganization. The nephrin adhesion protein is essential for the formation of actin-based foot processes in glomerular podocytes. The clustering of nephrin induces its tyrosine phosphorylation, Nck recruitment, and sustained localized actin polymerization. Any one of three phosphorylated (p)YDXV motifs on nephrin is sufficient to recruit Nck through its Src homology 2 (SH2) domain and induce localized actin polymerization at these clusters. Similarly, Nck SH3 mutants in which only the second or third SH3 domain is functional can mediate nephrin-induced actin polymerization. However, combining such nephrin and Nck mutants attenuates actin polymerization at nephrin-Nck clusters. We propose that the multiple Nck SH2-binding motifs on nephrin and the multiple SH3 domains of Nck act cooperatively to recruit the high local concentration of effectors at sites of nephrin activation that is required to initiate and maintain actin polymerization in vivo. We also find that YDXV motifs in the Tir protein of enteropathogenic *Escherichia coli* and nephrin are functionally interchangeable, indicating that Tir reorganizes the actin cytoskeleton by molecular mimicry of nephrin-like signaling. Together, these data identify pYDXV/Nck signaling as a potent and portable mechanism for physiological and pathological actin regulation.

Adaptor proteins, composed entirely of interaction domains, can link cell surface receptors to specific intracellular targets. The Nck family of adaptors is essential for early embryonic development in the mouse and functions in coupling phosphotyrosine (pTyr) signals to actin cytoskeletal reorganization (3). Mammals carry two related *Nck* genes, *Nck1* and *Nck2* (collectively termed "*Nck*"), each of which encodes a protein with three Src homology 3 (SH3) domains (SH3-1, -2, and -3) and a C-terminal SH2 domain (5, 20). Through its SH2 domain, Nck binds to specific pTyr-containing sites on activated receptors and scaffolds, and through its SH3 domains, Nck binds to proline-rich motifs in downstream effectors (6, 23). These latter targets include proteins involved in the control of cellular actin dynamics, such as N-WASP, WASP-interacting protein (WIP), PAK serine/threonine kinases, SPIN90, and dynamin (1, 2, 24, 29, 39). Indeed, artificially clustering the Nck SH3 domains at the plasma membrane induces actin polymerization (28).

In one physiological example, the Nck SH2 domain associates with nephrin, a transmembrane adhesion protein with eight extracellular immunoglobulin repeats and a short C-terminal cytoplasmic tail (Fig. 1A) (17, 22, 37). Nephrin is critical for the formation and maintenance of actin-dependent cellular protrusions known as foot processes, which are elaborated by specialized cells (termed podocytes) within the glomeruli of kidneys (32). Nephrin also anchors a specialized tight junction (the slit diaphragm) that forms between interdigitating foot processes of adjacent podocytes and is essential for the filtration barrier function of the glomeruli (Fig. 1A) (32). Loss-of-function mutations in the human gene encoding nephrin (*NPHS1*) cause defective actin organization in podocytes, foot process fusion (termed effacement), and proteinuria, resulting in a congenital nephrotic syndrome of the Finnish type (18); similar defects are seen in nephrin-deficient mice (26).

The nephrin cytoplasmic tail is phosphorylated on tyrosine residues by Src family kinases, both in vivo and in vitro, and in cell-based assays, this phosphorylation can be induced by the clustering of nephrin (17, 19, 21, 22, 38). Three sites of nephrin tyrosine phosphorylation are located in YDXV motifs, which correspond to a consensus binding site for the Nck SH2 domain (Fig. 1B) (11, 17, 22, 34, 37). The clustering of full-length nephrin or a CD16/7-nephrin chimeric protein leads to Nck recruitment through the phosphorylated YDXV sites and Nck-dependent actin polymerization (Fig. 1C) (17, 22, 37). As with nephrin, targeted deletion of *Nck2* in the podocytes of

* Corresponding author. Mailing address: Samuel Lunenfeld Research Institute, Mount Sinai Hospital, 1084-600 University Avenue, Toronto, Ontario M5G 1X5, Canada. Phone: (416) 586-8262. Fax: (416) 586-8869. E-mail: pawson@mshri.on.ca.
▽ Published ahead of print on 22 January 2008.

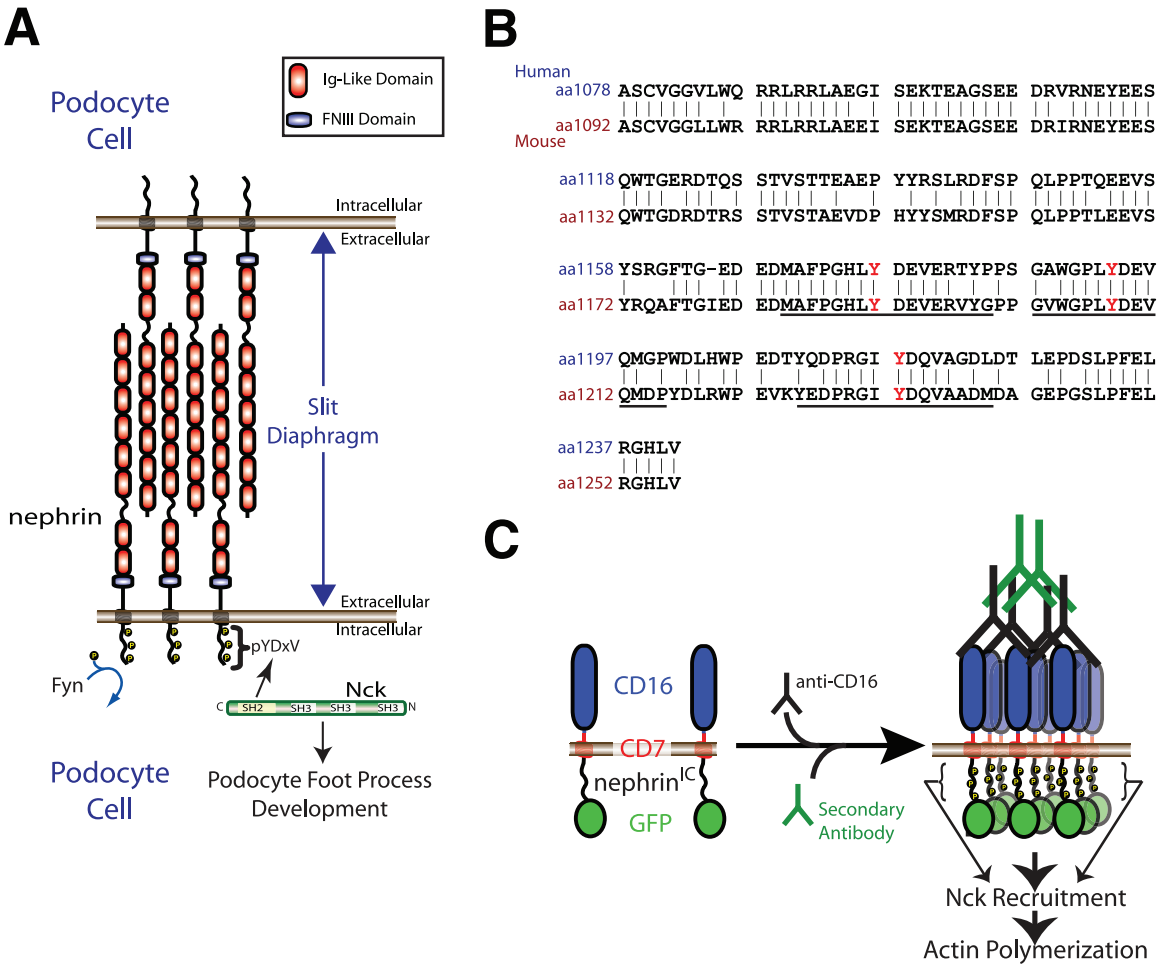

FIG. 1. (A) Nephrin is a transmembrane protein consisting of eight extracellular immunoglobulin (Ig)-like domains, a fibronectin type three (FNIII) domain, a transmembrane region, and an intracellular region. Nephrin is located at the slit diaphragm, where it interacts with nephrin molecules from adjacent foot processes of podocyte cells. Upon tyrosine phosphorylation by Fyn, nephrin recruits the adaptor protein Nck, which is required for proper foot process formation. (B) An alignment of the intracellular regions of human and mouse nephrin. The tyrosine residues located in the three YDXV motifs are shown (Y is shown in red). The sequences of the mouse peptides used for binding studies are underlined. Numbers to the left of the sequence denote amino acid residues. (C) A schematic of the CD16/7-nephrin^{IC} clustering system is shown. CD16/7-nephrin^{IC} fusion protein localizes to the plasma membrane in cells. Upon the addition of anti-CD16 antibodies to the cellular growth medium, the fusion protein clusters, causing nephrin^{IC} to become phosphorylated and recruit Nck, leading to localized polymerization of actin.

Nck1$^{-/-}$ mice leads to a failure in the formation of foot processes and proteinuria (17). Together, these data suggest that Nck adaptors link nephrin to the reorganization of the actin cytoskeleton in a fashion that is important for the architecture and function of podocytes.

Arguing for the importance of Nck in coupling pTyr signals to actin reorganization are the facts that pathogenic microorganisms, such as enteropathogenic *Escherichia coli* (EPEC) and vaccinia virus, have evolved related strategies to bind the Nck SH2 domain and thereby modify the actin cytoskeletons of infected cells (7, 12, 15). In a pathological context, EPEC recruits Nck by injecting a bacterially encoded protein, "translocated intimin receptor" (Tir), into the host cell (7, 15). Tir spans the plasma membrane twice, yielding an extracellular region that binds the intimin protein on the bacterial surface and two cytoplasmic tails that associate with regulatory proteins to induce ectopic actin-based structures termed pedestals (40). Tir is clustered through its association with intimin and is consequently phosphorylated by cytoplasmic tyrosine kinases, notably on Y474, which lies in an Nck SH2 domain recognition motif (YDEV) (7, 15). A Tir peptide encompassing phosphorylated Y474 binds the SH2 domains of Nck1 and Nck2 with high affinity in vitro (K_d between 100 and 300 nM) by engaging residues from the −2 to the +5 positions (8, 11, 15). The replacement of Y474 with phenylalanine or the inactivation of both *Nck* genes in infected cells markedly attenuates the ability of EPEC to induce actin-based pedestals, indicating that the recruitment of Nck to the phosphorylated (p)YDEV Tir site is important for the reorganization of host cell actin (7, 15).

Here, we have pursued the mechanisms through which adhesion proteins and Nck adaptors synergize to elicit potent and sustained reorganization of the actin cytoskeleton and we have explored the relationship between nephrin and EPEC Tir signaling.

MATERIALS AND METHODS

Plasmids. The construct consisting of the intracellular region of nephrin [referred to as CD16/7-nephrin(WT)^{IC}-GFP] and green fluorescent protein (GFP) and the CD16/7-nephrin(Y3F)^{IC}-GFP construct have previously been described (17). To generate CD16/7-nephrin(WT)^{IC}-*myc*, the intracellular domain of human nephrin was PCR amplified to generate an in-frame fusion with CD16/7, followed by a carboxy-terminal *myc* epitope tag. The CD16/7-nephrin(Y1193/1217F)^{IC}, CD16/7-nephrin(Y1176/1217F)^{IC}, and CD16/7-nephrin(Y1176/1193F)^{IC} constructs were generated by site-directed mutagenesis of CD16/7-nephrin(WT)^{IC}-GFP. The CD16/7-nephrin(Y3F)^{IC}-Tir-GFP construct was generated by amplifying nephrin(Y3F) with a primer to create the Tir peptide sequence PEEHIYDEVAADPG in frame with both the upstream nephrin(Y3F) and downstream GFP. Full-length human Nck1 (BC006403) cDNA (Open Biosystems) and Nck1 SH3-1^-,2^-,3^- (35) were PCR amplified and inserted into the Creator recombination system vector V180 containing an N-terminal triple-Flag tag (9). Nck1-*SH2*$^-$ (R308M); Nck1 *SH3-2*$^-$,*3*$^-$ (W143K and W229K); Nck1 *SH3-1*$^-$,*3*$^-$ (W38K and W229K); and Nck1 *SH3-1*$^-$,*2*$^-$ (W38K and W143K) were created by site-directed mutagenesis. The GFP-N-WASP construct has previously been described (16).

Tissue culture. All cells were grown in Dulbecco's modified Eagle's medium-high glucose supplemented with 10% fetal bovine serum. Mouse embryonic fibroblasts (MEFs) lacking both Nck1 and Nck2 have previously been described (3). Transient transfections in Nck-null MEFs were performed by using Effectene (Qiagen) and by following the manufacturer's guidelines. Transfections in HEK293T cells were performed using polyethyleneimine.

Antibody clustering experiments and cell imaging. A total of 1.0×10^5 MEFs were seeded onto glass coverslips in a six-well plate and transfected after 24 h. Twenty hours following transfection, the cells were incubated with 1 μg/ml of mouse monoclonal anti-CD16 (Sigma) or 0.5 μg/ml of anti-nephrin 50A9 (33) for 30 min (unless specified otherwise) at 37°C, washed once in Dulbecco's modified Eagle's medium with 10% fetal bovine serum, incubated with 1 μg/ml Alexa Fluor 488-conjugated goat anti-mouse secondary antibody (Molecular Probes) for 30 min (unless otherwise specified), and then fixed immediately in 4% paraformaldehyde and permeabilized. Staining for Flag-Nck was performed using a rabbit polyclonal anti-Flag antibody (Sigma), followed by Alexa Fluor 350-conjugated goat anti-rabbit secondary antibody (Molecular Probes). Filamentous actin was visualized with Texas Red-conjugated phalloidin (Molecular Probes). We performed staining of extracellular clusters by fixing the cells as described above and incubating them with a fluorescently labeled donkey anti-goat Texas Red-conjugated antibody without permeabilization. If stated, this was then followed by a second round of fixation, permeabilization, and then staining for F-actin as described above.

Cells were imaged using a Leica DMIRE2 fluorescence microscope (with Leica PL Fluotar 63×/0.70 objective) and a Hamamatsu C4742-95 charge-coupled device camera. Images were captured and processed using Openlab and Adobe Photoshop CS2 software.

Quantitation of actin polymerization. MEFs were seeded, stimulated, fixed, and stained as described above. Cells were visualized by using a Leica DMIRE2 fluorescence microscope (with Leica PL Fluotar 100×/1.30 oil objective). Cells that expressed both nephrin and Nck were scored for the presence of actin polymerization at nephrin clusters. All experiments were performed blind and were repeated at least four times. Cells which were scored positive usually contained more than 15 sites of actin polymerization, as seen at ×100 magnification.

Immunoprecipitations and immunoblotting. Immunoprecipitation and immunoblotting procedures have been described previously (17). Briefly, for phosphorylation analyses and coimmunoprecipitation experiments, cells were stimulated for 10 min at 37°C by using a 1 μg/ml dilution of anti-CD16 antibody. Lysates were prepared from transfected cells by using phospholipase C lysis buffer (50 mM HEPES, pH 7.5, 150 mM NaCl, 10% glycerol, 1% Triton X-100, 15 mM $MgCl_2$, 1 mM EGTA, 10 mM Na-PPi, 100 mM NaF) supplemented with fresh protease inhibitors. Commercially available antibodies used were as follows: monoclonal anti-Flag clone M2 (Sigma), monoclonal anti-pTyr clone 4G10 (Upstate), polyclonal anti-GFP 290 (Abcam), monoclonal anti-Nck (BD Pharmingen), and polyclonal anti-N-WASP H-100 (Santa Cruz).

Fluorescence polarization. Fluorescein-labeled peptides were synthesized as described previously (36) and purified by reverse-phase high-performance liquid chromatography. The identities of the fluorescein-labeled peptides were confirmed by mass spectrometry. Glutathione *S*-transferase (GST) fusions of Nck-SH2s were produced in *E. coli* strain BL21 CodonPlus (Stratagene) at 18°C overnight. Cells were centrifuged and disrupted in phosphate-buffered saline (PBS; pH 7.4) containing egg lysozyme (0.5 mg/ml; Sigma), complete protease inhibitor cocktail (Roche Applied Science), Triton X-100 (1%), and Benzonase (0.5 μl/ml; Novagen) for 10 min. The supernatants were passed over glutathione-Sepharose beads (Amersham Biosciences), which were then washed with PBS. Proteins were eluted using 20 mM reduced glutathione (EMD) and further purified using fast protein liquid chromatography in PBS. In the equilibrium binding studies, the fluorescein-labeled peptide probes were dissolved in PBS and an incremental amount of GST fusion proteins in PBS was added. The reaction mixtures were allowed to stand for 10 min at room temperature prior to measurements. All fluorescence polarization measurements were conducted at 22°C using a Beacon 2000 fluorescence polarization system (PanVera, Madison, WI) equipped with a 100-μl sample chamber. Results were analyzed using GraphPad Prism 3 software.

Bacterial strains. The following bacterial strains were used in this study: EPECΔ*tir* (14), EPECΔ*tir*/wtTir (14), EPECΔ*tir*/Tir Y474F (14), EPECΔ*tir*/Tir Y474F-nephrinY1217, and EPECΔ*tir*/Tir Y474F-nephrinY1217F (this study). To construct EPECΔ*tir*/Tir Y474F-nephrinY1217 and EPECΔ*tir*/Tir Y474F-nephrinY1217F, TirY474F in pACYC184 (10) was used as a template and PCR amplification was performed to make an in-frame fusion of TirY474F and nephrin amino acids 1212 to 1225. Following TOPO cloning (Invitrogen) and sequence verification, the amplified product was cloned into pACYC184. Following verification, the plasmid was introduced into EPECΔ*tir* by electroporation, followed by selection on chloramphenicol plates (30 μg/ml).

Immunofluorescence microscopy of EPEC. One milliliter of 2.5×10^4 HeLa cells was added to each well of a 24-well plate containing a 12-mm glass coverslip and grown overnight. Monolayers were infected with 0.5 μl of an overnight culture of the indicated bacterial strains and incubated for 3 h, followed by the addition of gentamicin (100 μg/ml) for 1 h. At this point, the concentration of gentamicin was reduced to 10 μg/ml, and incubation continued for an additional 2.5 h to promote pedestal elongation (31). Immunofluorescence microscopy and image analysis were performed as described previously (15) by using mouse monoclonal anti-Tir 2A8, mouse monoclonal anti-pTyr 4G10, and rabbit anti-EPEC, followed by Alexa Fluor 488- or 647-conjugated secondary antibodies (Molecular Probes). Filamentous actin was stained with Alexa Fluor 568-conjugated phalloidin (Molecular Probes). The cells were imaged on a Zeiss Axioplan2 epifluorescence microscope or an Olympus FV1000 confocal microscope using MetaMorph software.

RESULTS

Nephrin/Nck clusters induce sustained actin polymerization at the membrane. We analyzed the kinetics of Nck recruitment to nephrin and the consequent actin polymerization by clustering either a full-length human nephrin or a chimeric protein in which the extracellular domain of CD16 and the transmembrane domain of CD7 are fused to CD16/7-nephrin(WT)^{IC}. For this purpose, we used a MEF cell line derived from *Nck1*$^{-/-}$ *Nck2*$^{-/-}$ embryos that lack intrinsic Nck proteins (3). These cells were transfected with Flag-tagged Nck1 and CD16/7-nephrin(WT)^{IC} with GFP fused to the C terminus. Prior to the addition of clustering antibodies, both chimeric nephrin proteins and Flag-Nck1 were observed in diffuse localization patterns (Fig. 2A, row 1). The addition of anti-CD16 antibodies, followed by an Alexa Fluor 488 (green) secondary antibody, induced rapid clustering of CD16/7-nephrin(WT)^{IC} at the plasma membrane, with sites of nucleation appearing as early as 10 min poststimulation (5-min incubation with primary antibodies, followed by a 5-min incubation with secondary antibodies) (Fig. 2A, row 2). Both Nck and weak actin polymerization were also detected at these nucleation sites within 10 min, suggesting that a fraction of chimeric nephrin was functionally activated within this time frame (Fig. 2A, row 2). After 60 min of antibody stimulation, there was a strong increase in the amount of CD16/7-nephrin(WT)^{IC} located in clusters and a corresponding loss of diffusely localized protein (Fig. 2A, row 3). Concomitantly, Nck was more prominently coclustered with the chimeric nephrin protein at 60 min and actin polymeriza-

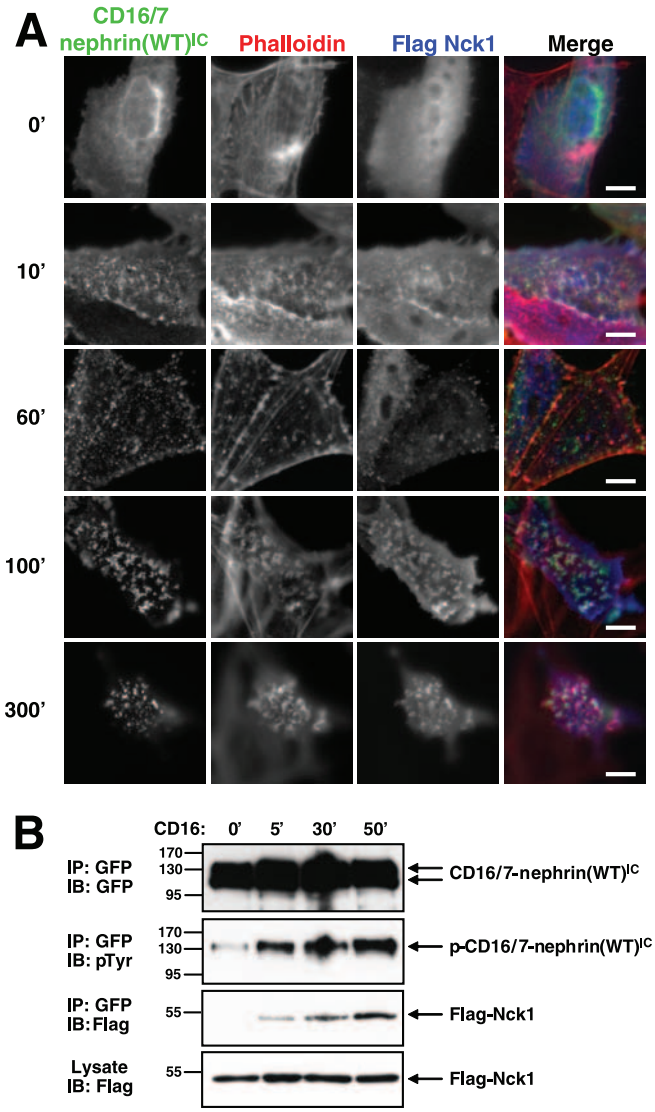

FIG. 2. CD16/7-nephrin(WT)^{IC} phosphorylation and Nck recruitment increases over time following antibody-induced clustering. (A) CD16/7-nephrin(WT)^{IC} was cotransfected with Flag-Nck1 into Nck-null MEFs. Anti-CD16 antibodies, followed by goat anti-mouse Alexa Fluor 488-conjugated antibody, were added to the cell growth medium to induce clustering for the indicated amounts of time (shown in minutes). Localization of nephrin (green), Nck (anti-Flag [blue]) and F-actin (phalloidin [red]) is shown. Scale bars = 10 μm. (B) GFP-tagged CD16/7-nephrin(WT)^{IC} was immunoprecipitated (IP) from cells clustered with anti-CD16 for the indicated time periods. Immunoprecipitates were immunoblotted (IB) with antibodies to GFP to identify CD16/7-nephrin(WT)^{IC} (top panel), anti-pTyr to identify tyrosine phosphorylated CD16/7-nephrin(WT)^{IC} (second panel), and anti-Flag to identify CD16/7-nephrin(WT)^{IC}-associated Nck1 (third panel). The bottom panel shows Nck1 levels in whole-cell lysates. The time of incubation with clustering antibodies is indicated above the panels.

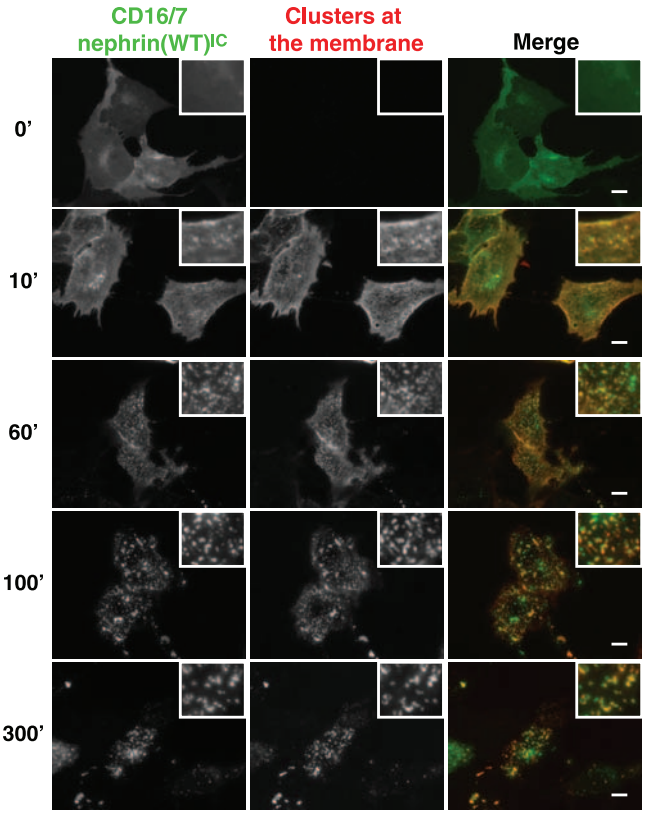

FIG. 3. Nephrin clusters are internalized. CD16/7-nephrin(WT)^{IC} was cotransfected with Flag-Nck1 into Nck-null MEFs. Anti-CD16 antibodies, followed by goat anti-mouse Alexa Fluor 488-conjugated antibodies (green), were added to the cell growth medium to induce clustering for the indicated amounts of time (shown in minutes). Cells were then fixed and stained with donkey anti-goat Texas Red-conjugated antibodies, in the absence of membrane permeabilization, to visualize extracellular clusters (shown in red). Yellow clusters represent nephrin present at the cellular membrane, while green clusters represent internalized nephrin. Scale bars = 10 μm.

tion emanating from these clusters was more robust (Fig. 2A, row 3). At 100 min of stimulation, the chimeric nephrin clusters had grown further, were associated with more intense Nck staining, and maintained polymerized actin (Fig. 2A, row 4). Both Nck and polymerized actin were still readily detected at clusters of CD16/7-nephrin(WT)^{IC} after 300 min (Fig. 2A, row 5). These experiments show that the activation of chimeric nephrin, the recruitment of Nck, and the polymerization of actin are initiated rapidly but also persist for an extended period. Similar results were observed with full-length human nephrin clustered with an antinephrin antibody (data not shown), suggesting that these are intrinsic functions of the nephrin cytoplasmic region and that the CD16/7-nephrin-(WT)^{IC} chimera is a valid surrogate for native nephrin in this assay. All subsequent experiments were performed with the CD16/7-nephrin(WT)^{IC} protein or mutants thereof.

Nephrin can be endocytosed upon clustering at the membrane (27). We therefore analyzed whether CD16/7-nephrin-(WT)^{IC} is internalized and whether actin polymerization occurs at internal sites. To this end, we stimulated cells expressing CD16/7-nephrin(WT)^{IC} with anti-CD16 antibodies, followed by Alexa Fluor 488-conjugated goat anti-mouse secondary antibodies (Fig. 3), for various periods of time. We then fixed the cells and stained them with Texas Red-conjugated donkey anti-goat antibodies in the absence of permeabilization in order to stain only nephrin clusters present at the membrane and exposed to the extracellular environment (Fig. 3). Under

these conditions, only internal CD16/7-nephrin(WT)^{IC} will be labeled green, whereas CD16/7-nephrin(WT)^{IC} clusters at the plasma membrane will appear yellow. This approach demonstrated that similar to the case for full-length nephrin, activated CD16/7-nephrin(WT)^{IC} clusters can be relocalized to intracellular structures (Fig. 3). Further staining of these cells with phalloidin revealed that the majority of nephrin-induced actin polymerization occurs at the plasma membrane, although a small number of internalized clusters also contain polymerized actin in their vicinities (data not shown). Taken together, these data indicate that the CD16/7-nephrin(WT)^{IC} clusters are dynamic, but that nephrin-induced actin polymerization occurs primarily at the plasma membrane.

To examine biochemically whether the amount of CD16/7-nephrin(WT)^{IC} phosphorylation and Flag-Nck1 recruitment increases over time following incubation with clustering antibodies, we performed Western blotting on lysates from cells that were stimulated with anti-CD16 antibodies for various periods (Fig. 2B). In unstimulated cells, we observed a small amount of CD16/7-nephrin(WT)^{IC} phosphorylation, but Flag-Nck1 was not detectably coprecipitated with nephrin. At 5 min of stimulation, there was a marked increase in CD16/7-nephrin(WT)^{IC} tyrosine phosphorylation and Flag-Nck1 was detected in CD16/7-nephrin(WT)^{IC} immunoprecipitates. Extending the time for which cells were incubated with anti-CD16 antibodies increased both the amount of CD16/7-nephrin-(WT)^{IC} tyrosine phosphorylation and its association with Flag-Nck1, consistent with the results obtained by fluorescence imaging of whole cells.

Nck recruitment to nephrin and localized actin polymerization requires a functional Nck SH2 domain. The association of Nck with nephrin involves the phosphorylation of three nephrin YDXV sites, each of which can bind the Nck SH2 domain in vitro (Fig. 1B) (17). We therefore tested whether the recruitment of Nck to nephrin clusters and the resulting actin polymerization are mediated by the Nck SH2 domain. To conduct the test, we mutated a conserved Arg required for pTyr recognition (R308 in the SH2 domain of Nck1) to Met (referred to as Nck1 *SH2*$^{-}$) (Fig. 4A). We then compared WT and *SH2*$^{-}$ Nck1 for their activities in the clustering assay, following transfection into *Nck1*$^{-/-}$ *Nck2*$^{-/-}$ MEFs, by scoring cells expressing both Flag-Nck1 and CD16/7-nephrin(WT)^{IC} for the presence of actin polymerization at nephrin clusters. WT Nck1 localized to CD16/7-nephrin(WT)^{IC} clusters and induced localized actin polymerization in 74.4% ± 8.9% (mean ± standard deviation) of cells (Fig. 2A, row 2, and 4D). In contrast, *SH2*$^{-}$ Nck1 did not localize to CD16/7-nephrin-(WT)^{IC} clusters, and did not induce significant actin polymerization (13.7% ± 5.6% of cells) (Nck1 *SH2*$^{-}$) (Fig. 4C and D). These results argue that Nck must be recruited to clusters through an SH2-pTyr interaction for nephrin to efficiently induce actin polymerization.

To determine whether SH2-mediated Nck recruitment to nephrin might influence its interactions with downstream effectors, we performed coimmunoprecipitation experiments using cells expressing Myc-tagged CD16/7-nephrin(WT)^{IC}, Flag-Nck1, and GFP-tagged N-WASP as potential Nck targets. Clustering the chimeric nephrin protein significantly increased the association of Nck1 with N-WASP over the basal level in unstimulated cells (Fig. 4B). However, this enhanced Nck/N-WASP interaction induced by nephrin clustering was not seen in cells expressing the Nck1 *SH2*$^{-}$ mutant (Fig. 4B). This is likely the result of an avidity effect produced by Nck clustering through nephrin, although the possibility that Nck undergoes conformational alterations cannot be excluded.

Nck SH2 domain binds individual phosphorylated YDXV nephrin motifs with similar affinities. To assess their relative potential to recruit Nck, we investigated the affinity with which each of the three pYDXV phosphopeptides from murine nephrin binds the Nck1 or Nck2 SH2 domains (for consistency, we used human numbering for the YDXV sites), using a fluorescence polarization binding assay. Both GST-Nck1 and GST-Nck2 SH2 domains bound to each of the pYDXV sites, with dissociation constants in the 1 μM range, with the exception of GST-Nck2 SH2 binding to nephrin pY1176, which showed a K_d of 0.46 ± 0.04 μM (Table 1). Similar affinities were observed for the GST-Nck1 SH2 and a His-tagged Nck1 SH2 domain binding to the nephrin pY1193 phosphopeptide (Table 1). The binding affinities of the GST-Nck1 and GST-Nck2 SH2 domains toward the pY474 peptide from the EPEC Tir protein were typically stronger than those observed for nephrin pYDXV sites, consistent with previously described values (Table 1) (11, 15). To determine whether the presence of multiple binding sites on a single peptide could increase the affinity for Nck SH2 domains, bisphosphorylated peptides were generated that encompassed the phosphorylated nephrin sites pY1176 and pY1193 (Table 1). The dissociation constants observed for both the GST-Nck1 domain and the GST-Nck2 SH2 domain for the doubly phosphorylated peptides were more than 10-fold stronger than those for the single sites. This result is likely due to an avidity effect caused by the dimerization of the GST moiety, as no difference in binding to the singly or doubly phosphorylated peptides was observed for the His-tagged Nck1 SH2 domain (Table 1).

Individual YDXV pTyr sites of nephrin can recruit Nck and induce actin polymerization. Mutation of all three YDXV tyrosine residues to phenylalanine [CD16/7-nephrin(Y3F)^{IC}] greatly reduces nephrin phosphorylation and suppresses Nck recruitment and actin polymerization at nephrin clusters (10.1% ± 1.6%) (Fig. 5A, B, and C) (17). However, as shown above, each individual site binds with relatively high affinity to the Nck SH2 domain. To investigate whether any individual YDXV pTyr site is sufficient for Nck recruitment and actin polymerization, double Y-to-F mutants in CD16/7-nephrin-(WT)^{IC} were created that leave only a single Nck YDXV motif in each protein. Immunoprecipitation and blotting experiments revealed that the extent of Nck interaction was reduced in these mutants compared to that in WT nephrin (Fig. 5A). However, all three mutants could still recruit Nck to clusters and induce localized actin polymerization, suggesting that each individual tyrosine residue is sufficient for actin polymerization mediated by WT Nck in this assay (the percentages of cells that showed actin polymerization at nephrin clusters were 75.5% ± 9.8% for Y1193/1217F, 67.1% ± 10.4% for Y1176/1217F, and 68.5% ± 4.8% for Y1176/1193F) (Fig. 5B and C).

Nephrin-induced actin polymerization requires the second or third SH3 domain of Nck. We also tested the roles of specific Nck SH3 domains in nephrin-induced actin polymerization. A mutant Nck1 protein with inactivating Trp-to-Lys substitutions in all three SH3 domains (*SH3-1*$^{-}$,*2*$^{-}$,*3*$^{-}$) (Fig.

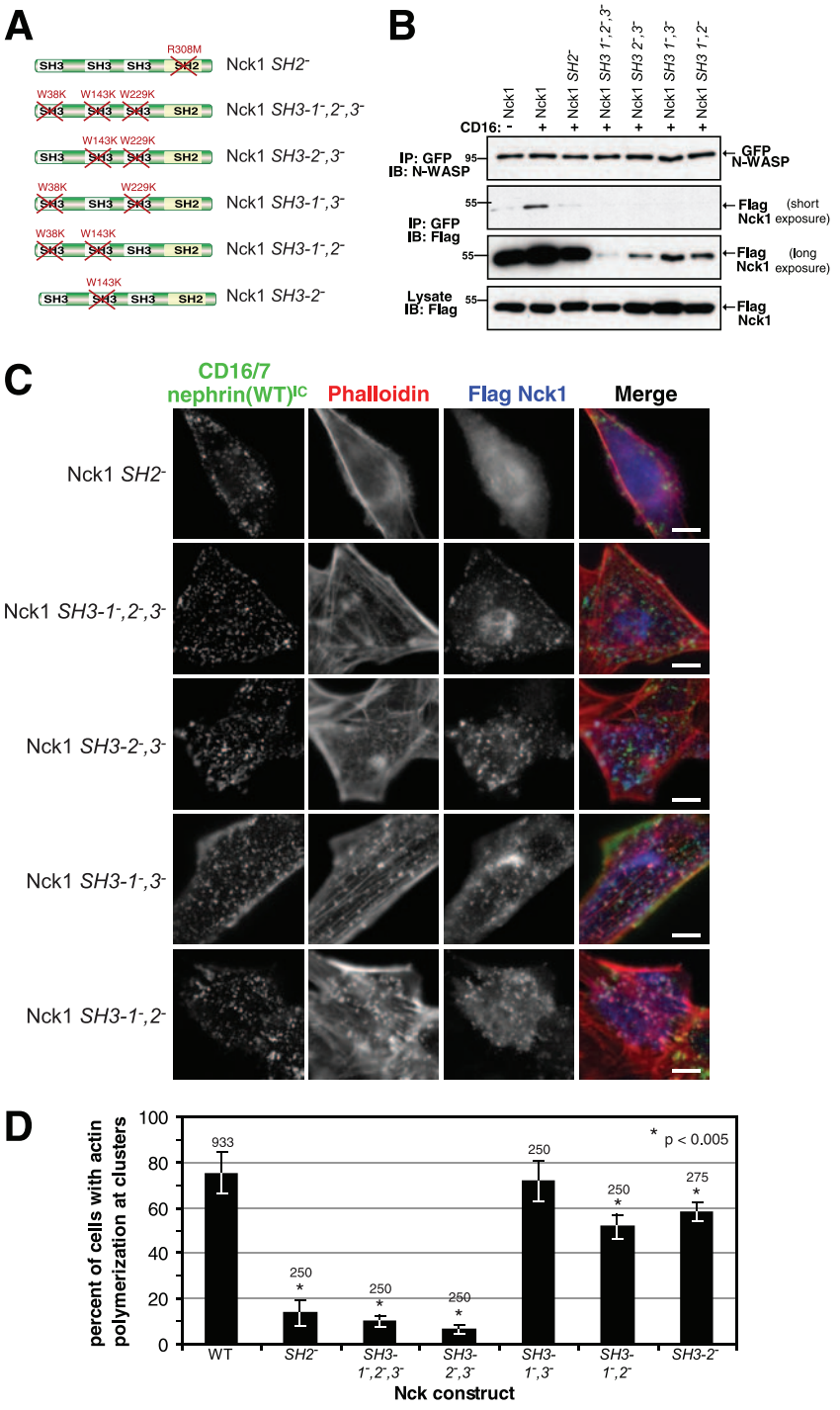

FIG. 4. Nephrin-induced actin polymerization is dependent on the SH2, SH3-2, and SH3-3 domains of Nck. (A) The SH2 and SH3 domains of Nck1 were rendered nonfunctional by specific amino acid substitutions. The various constructs used are depicted, with the mutations indicated in red. (B) Nck-null MEFs were cotransfected with *myc*-tagged CD16/7-nephrin(WT)^{IC}, GFP-tagged N-WASP, and either WT or mutant forms of Flag-Nck1, as indicated at the top of the panels. GFP-N-WASP was immunoprecipitated (IP) from cells expressing CD16/7-nephrin(WT)^{IC}-*myc*, either unclustered (−) or clustered with anti-CD16 antibodies for 10 min (+). Immunoprecipitates were immunoblotted (IB) with antibodies to N-WASP to identify GFP-N-WASP (top panel) and Flag to identify GFP-N-WASP-associated Nck1 proteins (middle panels). The middle panels show two different exposures of the same blot. The bottom panel shows Nck1 levels in whole-cell lysates. (C) Nck-null MEFs were cotransfected with GFP-tagged CD16/7-nephrin(WT)^{IC} and mutant forms of Flag-Nck1. Cells were incubated with anti-CD16 antibody for 30 min, followed by a 30-min incubation with goat anti-mouse Alexa Fluor 488 antibodies. The resulting localization of CD16/7-nephrin(WT)^{IC} (green), Flag-Nck (anti-Flag [blue]), and F-actin (phalloidin [red]) is shown. Scale bars = 10 μm. (D) Cells coexpressing GFP-tagged CD16/7-nephrin(WT)^{IC} with various Flag-Nck1 mutants were analyzed for the presence of actin polymerization at clusters. The numbers of cells that showed actin polymerization at CD16/7-nephrin(WT)^{IC} clusters were scored and are presented as percentages of total cells analyzed. Numbers above each bar indicate the total number of cells counted. Error bars represent standard deviations calculated from at least four independent experiments. Asterisks denote differences with statistical significance ($P < 0.005$) relative to the WT, as determined by the Student *t* test.

TABLE 1. Peptides binding affinities of Nck SH2 domains

Peptide	Sequence	K_d for[a]:			
		GST	GST-Nck1 SH2	GST-Nck2 SH2	His-Nck1 SH2
Nephrin Y1176	MAFPGHLpYDEVERVYG	–	1.30 ± 0.19	0.46 ± 0.04	–
Nephrin Y1193	GVWGPLpYDEVQMDP	NB	1.66 ± 0.36	1.60 ± 0.20	1.03 ± 0.12
Nephrin Y1217	YEDPRGIpYDQVAADM	–	1.05 ± 0.32	0.82 ± 0.06	–
Nephrin Y1176 + Y1193	GPGHLpYDEVERVYVWGPLpYDEVQMDP	NB	0.08 ± 0.01	0.04 ± 0.003	0.85 ± 0.06
Tir Y474	EEHIpYDEVAADP	–	0.13 ± 0.02	0.68 ± 0.12	–

[a] Values are expressed as μM ± standard error. –, not analyzed; NB, no binding.

4A) did not significantly coimmunoprecipitate with GFP-N-WASP (Fig. 4B), and it did not support localized actin polymerization upon clustering of CD16/7-nephrin(WT)^{IC} (10.2% ± 2.6%) (Fig. 4C and D). However, the *SH3-1*$^-$,*2*$^-$,*3*$^-$ Nck1 mutant protein was recruited to nephrin clusters, indicating that the binding of Nck to nephrin is not dependent on the SH3 domains (Fig. 4C). These observations demonstrate that the ability of Nck to recruit actin regulators through its SH3 domains is essential for nephrin-induced actin polymerization.

To ascertain which of the three Nck SH3 domains are active in the nephrin assay, we tested Nck1 mutant proteins in which two SH3 domains were inactivated and the proteins therefore had only a single functional SH3 domain (Fig. 4A). Nck1 *SH3-2*$^-$,*3*$^-$ (in which only the first SH3 domain is functional) interacted very weakly with GFP-N-WASP and did not induce actin polymerization at CD16/7-nephrin(WT)^{IC} clusters (6.3% ± 2.0%) (Fig. 4B, C, and D). In contrast, the Nck1 *SH3-1*$^-$,*3*$^-$ mutant (with only the SH3-2 domain intact) associated more strongly with GFP-N-WASP, albeit at a reduced level compared with that of WT Nck, and induced full actin polymerization at nephrin clusters (71.7% ± 8.9%) (Fig. 4B, C, and D). The Nck1 *SH3-1*$^-$,*2*$^-$ mutant (with only the SH3-3 domain intact) also mediated actin polymerization at nephrin clusters, although with lower efficiency (51.3% ± 5.2%), consistent with its reduced binding to GFP-N-WASP compared to that with Nck1 *SH3-1*$^-$,*3*$^-$ (Fig. 4B, C, and D). These results show that the SH3-2 and SH3-3 domains are individually sufficient to bind N-WASP and induce a degree of localized actin polymerization in response to nephrin clustering, whereas the SH3-1 domain is not. However, the efficiency of Nck1 association with N-WASP was significantly potentiated by the presence of multiple functional SH3 domains in the same Nck molecule. We did not observe any cooperative effect of the SH3-1 domain with the SH3-3 domain, since an *SH3-2*$^-$ Nck1 mutant (with functional SH3-1 and SH3-3 domains) showed no enhanced actin polymerization compared with that of a variant containing only a functional SH3-3 domain (58.1% ± 4.3%) (Nck1 *SH3-1*$^-$,*2*$^-$) (Fig. 4D).

Cooperative effects of multiple Nck SH2 domain-binding sites and Nck SH3 domains in nephrin-induced actin polymerization. We next investigated whether nephrin and Nck mutants that were individually sufficient to induce actin polymerization retained this activity when combined. We transfected Nck-null MEFs with Nck1 *SH3-1*$^-$,*3*$^-$ (the most active of the Nck mutants containing only a single functional SH3 domain) and each of the double-nephrin tyrosine mutants (Y1176/1193F, Y1176/1217F, and Y1193/1217F). All of these combinations were severely attenuated in their induction of localized actin polymerization (values were 21.8% ± 7.4% for Y1193/1217F, 22.8% ± 8.5% for Y1176/1217F, and 16.2% ± 7.5% for Y1176/1193F) (Fig. 6). These results indicate that while each individual nephrin YDXV phosphorylation site is minimally sufficient to induce actin polymerization when paired with three functional Nck SH3 domains and the individual SH3-2 domain is minimally sufficient to induce actin polymerization when paired with three functional nephrin YDXV motifs, actin polymerization is strongly reduced when each minimal element (a single nephrin YDXV motif and a single Nck SH3 domain) is paired in combination.

To determine whether the second and third SH3 domains of Nck can functionally complement one another when present on different Nck molecules, we cotransfected cells with Y1176/1217F mutant nephrin, Flag-Nck1 *SH3-1*$^-$,*3*$^-$, and Flag-Nck1 *SH3-1*$^-$,*2*$^-$. These cells did not show any increase in localized actin polymerization (21.0% ± 4.7%) compared to the level in cells expressing Y1176/1217F nephrin and Nck1 *SH3-1*$^-$,*3*$^-$ (Fig. 6). This result demonstrates that the second and third SH3 domains of Nck cannot function in *trans* to restore localized actin polymerization at Y1176/1217F nephrin clusters. Taken together, these results suggest that oligomerization of the signaling proteins downstream of nephrin may be important in transmitting a signal for efficient actin polymerization.

The Nck SH2 binding motifs of nephrin and Tir are functionally interchangeable. The Tir protein of EPEC has an Nck SH2 binding site (Y474) that is required for pedestal formation induced at the sites of bacterial attachment (7, 15). The Tir Y474 site has a core YDXV sequence, although it employs a more extended motif to engage the Nck SH2 domain (11). We have proposed that EPEC Tir has evolved to mimic Nck SH2 domain-binding sites, such as those found on nephrin (17). To test this theory, we generated a nephrin variant in which a 14-amino-acid peptide encompassing the Tir Y474 site is fused to the intracellular region of CD16/7-nephrin(Y3F)^{IC} (Fig. 7A). The only YDXV site in this protein is therefore provided by the motif engrafted from EPEC Tir. While CD16/7-nephrin(Y3F)^{IC} was inactive (Fig. 5B), the incorporation of the Tir Nck SH2-binding motif was sufficient to rescue Nck recruitment and actin polymerization at nephrin clusters (Fig. 7B). We also tested whether the Y^{1217}DQV site of human nephrin could rescue the Tir Y474F mutant, which fails to recruit Nck and induce efficient actin pedestal formation upon bacterial infection (Fig. 7C). We therefore engineered an EPEC bacterium that encodes a Tir Y474F protein to which is fused a 14-amino-acid peptide containing the human nephrin Y^{1217}DQV site (Fig. 7A and C). As anticipated, WT EPEC induced prominent Tir-dependent tyrosine phosphorylation

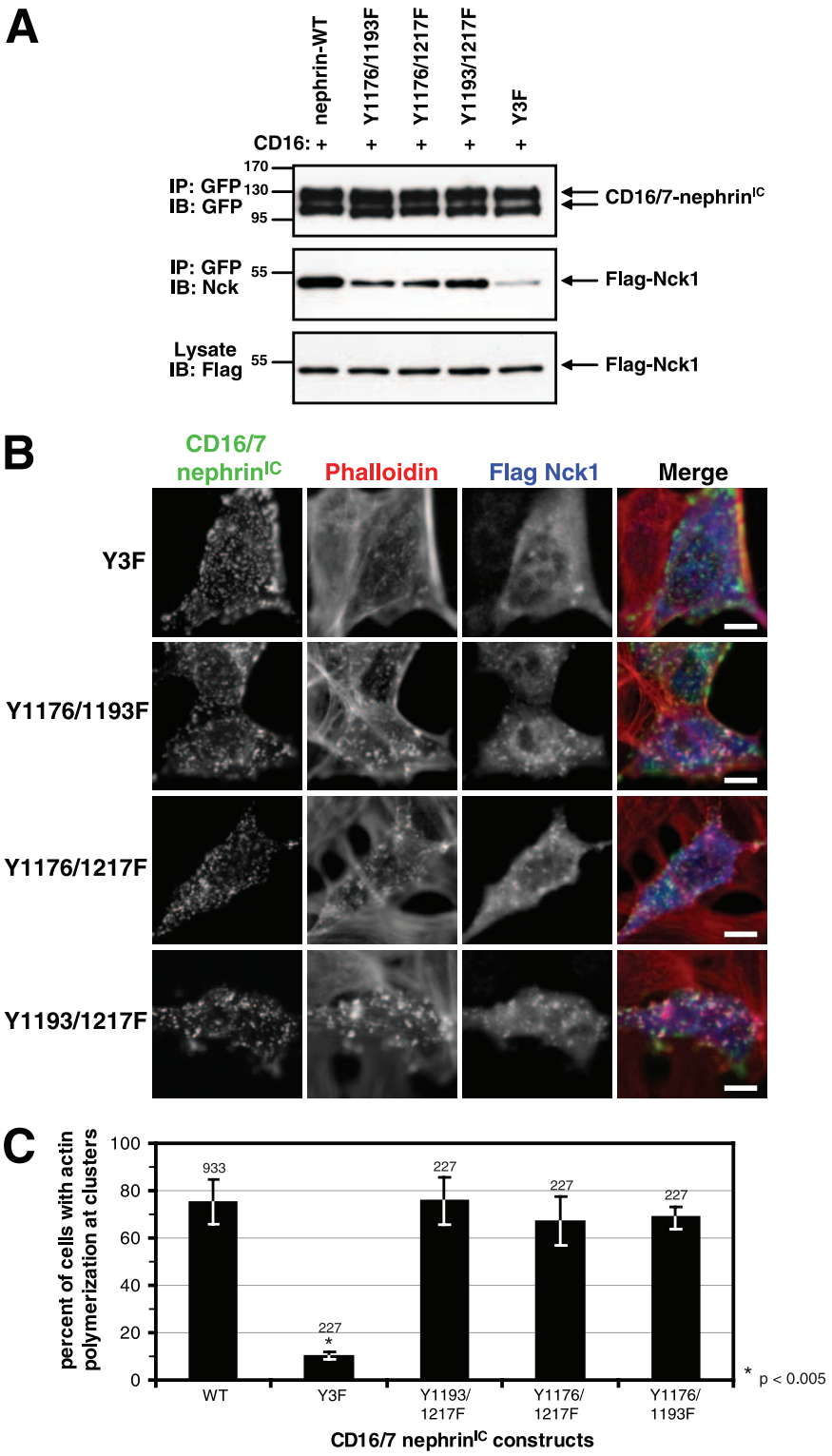

FIG. 5. A single YDXV motif on nephrin is sufficient to recruit Nck and induce actin polymerization. (A) Nck-null MEFs were transfected with either GFP-tagged CD16/7-nephrin(WT)^{IC} or mutants with two or three nephrin YDXV tyrosine residues mutated to phenylalanine as indicated, together with WT Flag-Nck1. Cells were incubated with anti-CD16 antibodies for 10 min (+). GFP-tagged CD16/7-nephrin(WT)^{IC} was immunoprecipitated (IP), and immunoprecipitates were immunoblotted (IB) with antibodies to GFP to identify CD16/7-nephrin(WT)^{IC} (top panel) and Nck to identify CD16/7-nephrin^{IC}-associated Flag-Nck1 (middle panel). The bottom panel shows Flag-Nck1 levels in whole-cell lysates. (B) Cells were transfected as for panel A, and GFP-tagged CD16/7-nephrin^{IC} mutants were clustered with anti-CD16 antibodies for 30 min, followed by clustering with goat anti-mouse Alexa Fluor 488-conjugated antibodies for 30 min. Immunofluorescence localization of GFP-tagged CD16/7-nephrin^{IC} mutants (green), Flag-Nck (anti-Flag [blue]), and F-actin (phalloidin [red]) is shown. Scale bars = 10 μm. (C) Cells expressing both Flag-Nck1 and GFP-tagged CD16/7-nephrin^{IC} (WT or mutants) were analyzed for the presence of actin polymerization at clusters. The numbers of cells that showed actin polymerization at CD16/7-nephrin^{IC} clusters were scored and are presented as percentages of total cells analyzed. Numbers above bars indicate the total numbers of cells counted. Error bars represent standard deviations calculated from at least four independent experiments. Asterisks denote differences with statistical significance ($P < 0.005$) relative to the WT, as determined by the Student t test.

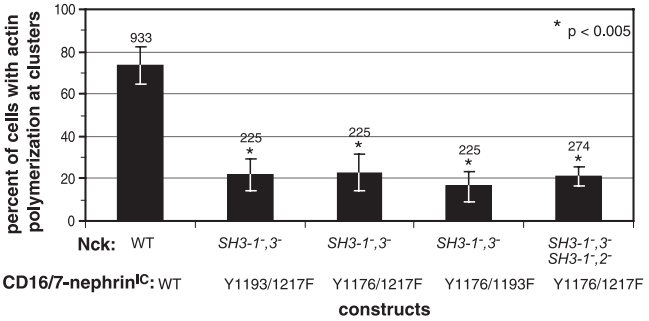

FIG. 6. Combining nephrin and Nck mutants suppresses localized actin polymerization. Cells coexpressing Flag-Nck1 and CD16/7-nephrin^{IC} were analyzed for the presence of actin polymerization at clusters. The various combinations of nephrin and Nck1 mutants are indicated. The numbers of cells that showed actin polymerization at CD16/7-nephrin^{IC} clusters were scored and are presented as percentages of total cells counted. Numbers above bars indicate the total numbers of cells counted. Error bars represent standard deviations calculated from at least four independent experiments. Asterisks denote differences with statistical significances ($P < 0.005$) relative to the WT, as determined by the Student t test.

and actin polymerization at sites of bacterial attachment, which were attenuated in EPEC encoding a Tir Y474F mutant (Fig. 7C). These defects were rescued by incorporating the 14-residue nephrin Y1217 motif into the Tir Y474F mutant, but they were not rescued by the corresponding protein in which the Tyr1217 was changed to phenylalanine. The motif encompassing the nephrin Y^{1217}DQV site is therefore sufficient to promote actin pedestal formation by EPEC Tir in the context of bacterial infection (Fig. 7C). Tir expression was verified in all strains by staining EPEC-infected cells with anti-Tir antibodies (data not shown). These data argue that EPEC Tir manipulates the cytoskeletons of infected cells through a process of molecular mimicry.

DISCUSSION

We have investigated the mechanisms by which the adhesive protein nephrin exploits Nck SH2/SH3 adaptors to induce localized actin polymerization. We find that the pTyr-binding activity of the Nck1 SH2 domain is required for Nck recruitment to clustered nephrin and localized actin polymerization at membrane nephrin clusters. Mutations that simultaneously inactivate all three SH3 domains did not block Nck recruitment to activated nephrin, but the mutations inhibited nephrin-induced actin polymerization. These data support a model in which Nck functions as an adaptor to link phosphorylated nephrin to downstream targets involved in actin polymerization.

Nephrin has three YDXV motifs, each of which can bind the SH2 domain of Nck1 or Nck2 with K_ds of ~1 μM, and Nck has three SH3 domains; our results indicate several levels at which these motifs and domains may act cooperatively to stimulate actin reorganization. For example, the recruitment of Nck to the phosphorylated nephrin tail is associated with an increased association of Nck with N-WASP, which might potentiate the local concentration of N-WASP in the vicinity of activated nephrin. In this regard, a single N-WASP molecule has 68 proline residues in a 116-amino-acid sequence and might therefore have sufficient SH3-binding sites to simultaneously accommodate multiple Nck molecules. Although the SH3-2 and SH3-3 domains of Nck are individually able to associate with N-WASP in cells, they do so at a much reduced level compared with that of the multiple SH3 domains present in WT Nck, indicating that the SH3 domains within a single Nck chain synergize in binding to N-WASP. In contrast, polymerized actin does not appear to have an effect on Nck binding to N-WASP as no decrease in the interaction of Nck with N-WASP is observed upon treatment of cells with cytochalasin D prior to nephrin clustering (data not shown).

In addition to these biochemical observations, our analysis of nephrin and Nck mutants suggests a functional cooperativity between the multiple nephrin pYDXV motifs and Nck SH3 domains. Any one of the YDXV sites of human nephrin is sufficient for Nck recruitment and consequent actin polymerization at CD16/7-nephrin^{IC} clusters in MEFs expressing WT Nck. Similarly, the second or third SH3 domain of Nck is individually capable of mediating actin polymerization in response to WT nephrin with three YDXV sites, albeit with reduced efficiency in the case of SH3-3. Previous work has suggested that all three Nck SH3 domains are required to induce actin polymerization, and our results indicate that multiple SH3 domains are essential in specific contexts; the difference may be in the distinct mechanisms employed for activation of the Nck SH3 domains (28). Our results are consistent with the binding profiles of the Nck SH3 domains, since the second and third SH3 domains associate with the majority of Nck targets implicated in cytoskeletal regulation (6, 23). For example, the SH3-2 and SH3-3 domains of Nck can both bind to N-WASP and the SH3-2 domain also binds WIP and PAK (1, 4, 29, 30). Potentially, the recruitment of either N-WASP or WIP is sufficient to form an N-WASP-WIP complex that induces actin polymerization (25).

Although a single nephrin YDXV motif or Nck SH3 domain is sufficient to induce actin polymerization in MEFs following nephrin clustering, a combination of a nephrin mutant with only one YDXV motif and an Nck mutant with only a single functional SH3 domain (SH3-2) is relatively inactive. This cooperative function of the multiple nephrin YDXV motifs and Nck SH3 domains could be explained if a high local concentration of Nck targets were being generated, and thus, a network of cross-linked effector proteins is important for potent actin polymerization induced by nephrin. SH3-mediated interactions could also affect the stability of the Nck-nephrin complex. For example, if two Nck molecules bind through their SH3 domains to the same effector molecule (such as the extended proline-rich region in N-WASP), the affinities of their SH2 domains for multiply phosphorylated nephrin could increase through an avidity effect, as occurs in vitro for Nck SH2 domains dimerized with GST.

The multiple pYDXV motifs and SH3 domains of the nephrin-Nck cluster could therefore enhance the oligomerization of effectors and also stabilize the nephrin-Nck complex. In podocytes, this may be important for converting initially weak signals at the developing and mature slit diaphragm into a strong and sustained actin response required to form and maintain foot processes and, thus, the filtration apparatus of the glomerulus in the kidney. The notion that multiple pTyr-SH2 domain interactions may cooperate at the slit diaphragm to

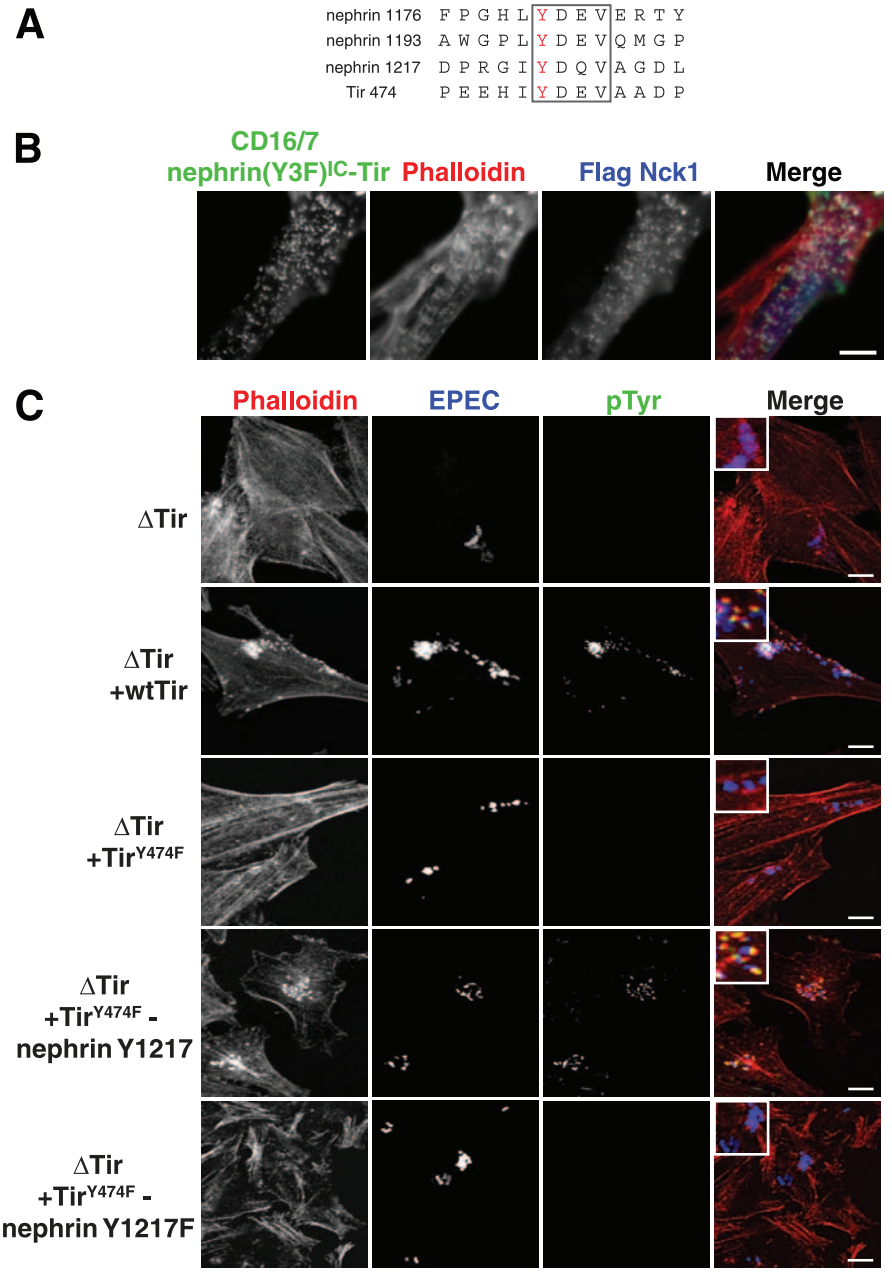

FIG. 7. The YDXV motifs of the EPEC Tir protein and nephrin are functionally interchangeable. (A) An alignment of the sequences encompassing the YDXV motifs (boxed) of nephrin and EPEC Tir is shown. The phosphorylated Tyr is colored red. Numbers to the left of the sequence indicate the amino acid numbers of the indicated Tyr residue. (B) Nck-null MEFs were cotransfected with GFP-tagged CD16/7-nephrin(Y3F)^{IC}-Tir and Flag-Nck1 and incubated with anti-CD16 antibodies for 30 min, followed by a 30-min incubation with goat anti-mouse Alexa Fluor 488-conjugated antibodies. Immunofluorescence localization of CD16/7-nephrin(Y3F)^{IC}-Tir (green), Flag-Nck1 (anti-Flag [blue]), and F-actin (phalloidin [red]) is shown. (C) HeLa cells were infected with various strains of EPEC, either without Tir (ΔTir) or with ΔTir reconstituted with WT Tir, Tir^{Y474F}, Tir^{Y474F}-nephrin Y1217, or Tir^{Y474F}-nephrin Y1217F. The EPEC bacteria were visualized with anti-EPEC (blue), sites of tyrosine phosphorylation were visualized with anti-pTyr antibodies (green), and polymerized actin was visualized with phalloidin (red). Bacteria lacking Tir (ΔTir) are impaired in their abilities to adhere to host cells and, thus, show reduced levels of staining for EPEC. Scale bars = 10 μm.

induce actin polymerization is supported by the finding that Neph1, a transmembrane protein that associates with nephrin, is tyrosine phosphorylated upon clustering and associates with the Grb2 adaptor (13). Coclustering of nephrin with Neph1, which further increases the number of pTyr residues and SH3 domains present in the complex, induces levels of actin polymerization that are higher than those observed with either receptor alone, potentially by enhancing the link between nephrin and Nck effectors, such as N-WASP (13).

We have previously proposed that the EPEC Tir protein polymerizes actin at sites of bacterial attachment by mimicking this pYDXV-based nephrin signaling. In support of this no-

tion, we find that a 14-residue motif encompassing the Y^{474}DEV site from Tir will restore actin polymerizing activity to a nephrin mutant that lacks all three intrinsic YDXV motifs. Conversely, grafting a 14-amino-acid element containing the Y^{1217}DQV site from human nephrin onto a Tir Y474F mutant restores the ability of EPEC to efficiently induce actin-based pedestals in infected cells. EPEC Tir may require only a single high-affinity Nck-binding site because of the very extensive clustering of Tir induced by the intimin protein on the bacterial surface. The acquisition of short signaling motifs that engage specific components of the intracellular machinery therefore represents a facile way in which pathogens can evolve to modify cellular behavior.

In combination, our data suggest that clustering of adhesion proteins and consequent pYDXV/Nck signaling, likely operating through the oligomerization of cytoplasmic effectors, are a portable and potent mechanism for physiological and pathological actin regulation.

ACKNOWLEDGMENTS

We are indebted to Karl Tryggvason for 50A9 antinephrin antibodies, Bruce Mayer for the original Nck1 *SH3-1*$^{-}$,*2*$^{-}$,*3*$^{-}$ construct, and Peter McPherson for the GFP-N-WASP construct. We thank Rick Bagshaw, Jerry Gish, Sarang Kulkarni, David Schibli, Neil Warner, and Chenggang Wu for technical assistance and Jerry Gish, Giselle Wiggin, and Rick Bagshaw for their help in preparing the manuscript. I.M.B. thanks G. C. Leung for her assistance, support, and insights.

Work in our laboratories was funded by the Canadian Institute for Health Research (CIHR) (to T.P., S.G., and S.S.C.L.), Genome Canada (to S.S.C.L. and T.P.) with funds provided through the Ontario Genomics Institute, and the Kidney Foundation of Canada (to N.J.). S.E.Q. holds a Canadian Research Chair in Vascular and Metabolic Biology. S.S.C.L. holds a Canada Research Chair in Functional Genomics and Cellular Proteomics. S.G. holds a Canadian Research Chair in Bacterial Pathogenesis. N.J. is the recipient of a Natural Sciences and Engineering Research Council of Canada University Faculty Award. T.P. is a distinguished scientist of the CIHR.

REFERENCES

1. **Anton, I. M., W. Lu, B. J. Mayer, N. Ramesh, and R. S. Geha.** 1998. The Wiskott-Aldrich syndrome protein-interacting protein (WIP) binds to the adaptor protein Nck. J. Biol. Chem. **273:**20992–20995.
2. **Bagrodia, S., S. J. Taylor, C. L. Creasy, J. Chernoff, and R. A. Cerione.** 1995. Identification of a mouse p21Cdc42/Rac activated kinase. J. Biol. Chem. **270:**22731–22737.
3. **Bladt, F., E. Aippersbach, S. Gelkop, G. A. Strasser, P. Nash, A. Tafuri, F. B. Gertler, and T. Pawson.** 2003. The murine Nck SH2/SH3 adaptors are important for the development of mesoderm-derived embryonic structures and for regulating the cellular actin network. Mol. Cell. Biol. **23:**4586–4597.
4. **Bokoch, G. M., Y. Wang, B. P. Bohl, M. A. Sells, L. A. Quilliam, and U. G. Knaus.** 1996. Interaction of the Nck adapter protein with p21-activated kinase (PAK1). J. Biol. Chem. **271:**25746–25749.
5. **Braverman, L. E., and L. A. Quilliam.** 1999. Identification of Grb4/Nckbeta, a src homology 2 and 3 domain-containing adapter protein having similar binding and biological properties to Nck. J. Biol. Chem. **274:**5542–5549.
6. **Buday, L., L. Wunderlich, and P. Tamas.** 2002. The Nck family of adapter proteins: regulators of actin cytoskeleton. Cell. Signal. **14:**723–731.
7. **Campellone, K. G., A. Giese, D. J. Tipper, and J. M. Leong.** 2002. A tyrosine-phosphorylated 12-amino-acid sequence of enteropathogenic Escherichia coli Tir binds the host adaptor protein Nck and is required for Nck localization to actin pedestals. Mol. Microbiol. **43:**1227–1241.
8. **Campellone, K. G., S. Rankin, T. Pawson, M. W. Kirschner, D. J. Tipper, and J. M. Leong.** 2004. Clustering of Nck by a 12-residue Tir phosphopeptide is sufficient to trigger localized actin assembly. J. Cell Biol. **164:**407–416.
9. **Colwill, K., C. D. Wells, K. Elder, M. Goudreault, K. Hersi, S. Kulkarni, W. R. Hardy, T. Pawson, and G. B. Morin.** 2006. Modification of the Creator recombination system for proteomics applications—improved expression by addition of splice sites. BMC Biotechnol. **6:**13.
10. **DeVinney, R., J. L. Puente, A. Gauthier, D. Goosney, and B. B. Finlay.** 2001. Enterohaemorrhagic and enteropathogenic Escherichia coli use a different Tir-based mechanism for pedestal formation. Mol. Microbiol. **41:**1445–1458.
11. **Frese, S., W. D. Schubert, A. C. Findeis, T. Marquardt, Y. S. Roske, T. E. Stradal, and D. W. Heinz.** 2006. The phosphotyrosine peptide binding specificity of Nck1 and Nck2 Src homology 2 domains. J. Biol. Chem. **281:**18236–18245.
12. **Frischknecht, F., V. Moreau, S. Rottger, S. Gonfloni, I. Reckmann, G. Superti-Furga, and M. Way.** 1999. Actin-based motility of vaccinia virus mimics receptor tyrosine kinase signalling. Nature **401:**926–929.
13. **Garg, P., R. Verma, D. Nihalani, D. B. Johnstone, and L. B. Holzman.** 2007. Neph1 cooperates with nephrin to transduce a signal that induces actin polymerization. Mol. Cell. Biol. **27:**8698–8712.
14. **Gauthier, A., M. de Grado, and B. B. Finlay.** 2000. Mechanical fractionation reveals structural requirements for enteropathogenic *Escherichia coli* Tir insertion into host membranes. Infect. Immun. **68:**4344–4348.
15. **Gruenheid, S., R. DeVinney, F. Bladt, D. Goosney, S. Gelkop, G. D. Gish, T. Pawson, and B. B. Finlay.** 2001. Enteropathogenic E. coli Tir binds Nck to initiate actin pedestal formation in host cells. Nat. Cell Biol. **3:**856–859.
16. **Hussain, N. K., S. Jenna, M. Glogauer, C. C. Quinn, S. Wasiak, M. Guipponi, S. E. Antonarakis, B. K. Kay, T. P. Stossel, N. Lamarche-Vane, and P. S. McPherson.** 2001. Endocytic protein intersectin-l regulates actin assembly via Cdc42 and N-WASP. Nat. Cell Biol. **3:**927–932.
17. **Jones, N., I. M. Blasutig, V. Eremina, J. M. Ruston, F. Bladt, H. Li, H. Huang, L. Larose, S. S. Li, T. Takano, S. E. Quaggin, and T. Pawson.** 2006. Nck adaptor proteins link nephrin to the actin cytoskeleton of kidney podocytes. Nature **440:**818–823.
18. **Kestila, M., U. Lenkkeri, M. Mannikko, J. Lamerdin, P. McCready, H. Putaala, V. Ruotsalainen, T. Morita, M. Nissinen, R. Herva, C. E. Kashtan, L. Peltonen, C. Holmberg, A. Olsen, and K. Tryggvason.** 1998. Positionally cloned gene for a novel glomerular protein—nephrin—is mutated in congenital nephrotic syndrome. Mol. Cell **1:**575–582.
19. **Lahdenpera, J., P. Kilpelainen, X. L. Liu, T. Pikkarainen, P. Reponen, V. Ruotsalainen, and K. Tryggvason.** 2003. Clustering-induced tyrosine phosphorylation of nephrin by Src family kinases. Kidney Int. **64:**404–413.
20. **Lehmann, J. M., G. Riethmuller, and J. P. Johnson.** 1990. Nck, a melanoma cDNA encoding a cytoplasmic protein consisting of the src homology units SH2 and SH3. Nucleic Acids Res. **18:**1048.
21. **Li, H., S. Lemay, L. Aoudjit, H. Kawachi, and T. Takano.** 2004. SRC-family kinase Fyn phosphorylates the cytoplasmic domain of nephrin and modulates its interaction with podocin. J. Am. Soc. Nephrol. **15:**3006–3015.
22. **Li, H., J. Zhu, L. Aoudjit, M. Latreille, H. Kawachi, L. Larose, and T. Takano.** 2006. Rat nephrin modulates cell morphology via the adaptor protein Nck. Biochem. Biophys. Res. Commun. **349:**310–316.
23. **Li, W., J. Fan, and D. T. Woodley.** 2001. Nck/Dock: an adapter between cell surface receptors and the actin cytoskeleton. Oncogene **20:**6403–6417.
24. **Lim, C. S., E. S. Park, D. J. Kim, Y. H. Song, S. H. Eom, J. S. Chun, J. H. Kim, J. K. Kim, D. Park, and W. K. Song.** 2001. SPIN90 (SH3 protein interacting with Nck, 90 kDa), an adaptor protein that is developmentally regulated during cardiac myocyte differentiation. J. Biol. Chem. **276:**12871–12878.
25. **Moreau, V., F. Frischknecht, I. Reckmann, R. Vincentelli, G. Rabut, D. Stewart, and M. Way.** 2000. A complex of N-WASP and WIP integrates signalling cascades that lead to actin polymerization. Nat. Cell Biol. **2:**441–448.
26. **Putaala, H., R. Soininen, P. Kilpelainen, J. Wartiovaara, and K. Tryggvason.** 2001. The murine nephrin gene is specifically expressed in kidney, brain and pancreas: inactivation of the gene leads to massive proteinuria and neonatal death. Hum. Mol. Genet. **10:**1–8.
27. **Quack, I., L. C. Rump, P. Gerke, I. Walther, T. Vinke, O. Vonend, T. Grunwald, and L. Sellin.** 2006. β-Arrestin2 mediates nephrin endocytosis and impairs slit diaphragm integrity. Proc. Natl. Acad. Sci. USA **103:**14110–14115.
28. **Rivera, G. M., C. A. Briceno, F. Takeshima, S. B. Snapper, and B. J. Mayer.** 2004. Inducible clustering of membrane-targeted SH3 domains of the adaptor protein Nck triggers localized actin polymerization. Curr. Biol. **14:**11–22.
29. **Rivero-Lezcano, O. M., A. Marcilla, J. H. Sameshima, and K. C. Robbins.** 1995. Wiskott-Aldrich syndrome protein physically associates with Nck through Src homology 3 domains. Mol. Cell. Biol. **15:**5725–5731.
30. **Rohatgi, R., P. Nollau, H. Y. Ho, M. W. Kirschner, and B. J. Mayer.** 2001. Nck and phosphatidylinositol 4,5-bisphosphate synergistically activate actin polymerization through the N-WASP-Arp2/3 pathway. J. Biol. Chem. **276:**26448–26452.
31. **Rosenshine, I., S. Ruschkowski, M. Stein, D. J. Reinscheid, S. D. Mills, and B. B. Finlay.** 1996. A pathogenic bacterium triggers epithelial signals to form a functional bacterial receptor that mediates actin pseudopod formation. EMBO J. **15:**2613–2624.
32. **Ruotsalainen, V., P. Ljungberg, J. Wartiovaara, U. Lenkkeri, M. Kestila, H. Jalanko, C. Holmberg, and K. Tryggvason.** 1999. Nephrin is specifically located at the slit diaphragm of glomerular podocytes. Proc. Natl. Acad. Sci. USA **96:**7962–7967.
33. **Ruotsalainen, V., J. Patrakka, P. Tissari, P. Reponen, M. Hess, M. Kestila, C. Holmberg, R. Salonen, M. Heikinheimo, J. Wartiovaara, K. Tryggvason, and H. Jalanko.** 2000. Role of nephrin in cell junction formation in human nephrogenesis. Am. J. Pathol. **157:**1905–1916.

34. **Songyang, Z., S. E. Shoelson, M. Chaudhuri, G. Gish, T. Pawson, W. G. Haser, F. King, T. Roberts, S. Ratnofsky, R. J. Lechleider, et al.** 1993. SH2 domains recognize specific phosphopeptide sequences. Cell **72:**767–778.
35. **Tanaka, M., R. Gupta, and B. J. Mayer.** 1995. Differential inhibition of signaling pathways by dominant-negative SH2/SH3 adapter proteins. Mol. Cell. Biol. **15:**6829–6837.
36. **van der Geer, P., S. Wiley, G. D. Gish, V. K. Lai, R. Stephens, M. F. White, D. Kaplan, and T. Pawson.** 1996. Identification of residues that control specific binding of the Shc phosphotyrosine-binding domain to phosphotyrosine sites. Proc. Natl. Acad. Sci. USA **93:**963–968.
37. **Verma, R., I. Kovari, A. Soofi, D. Nihalani, K. Patrie, and L. B. Holzman.** 2006. Nephrin ectodomain engagement results in Src kinase activation, nephrin phosphorylation, Nck recruitment, and actin polymerization. J. Clin. Investig. **116:**1346–1359.
38. **Verma, R., B. Wharram, I. Kovari, R. Kunkel, D. Nihalani, K. K. Wary, R. C. Wiggins, P. Killen, and L. B. Holzman.** 2003. Fyn binds to and phosphorylates the kidney slit diaphragm component Nephrin. J. Biol. Chem. **278:** 20716–20723.
39. **Wunderlich, L., A. Farago, and L. Buday.** 1999. Characterization of interactions of Nck with Sos and dynamin. Cell. Signal. **11:**25–29.
40. **Zaharik, M. L., S. Gruenheid, A. J. Perrin, and B. B. Finlay.** 2002. Delivery of dangerous goods: type III secretion in enteric pathogens. Int. J. Med. Microbiol. **291:**593–603.